Indian Journal of Chemistry
Vol. 56A, June 2017, pp. 626-632

Tautomerism and non-covalent interactions of flucytosine with armchair (5,5) SWCNT and γ-Fe_2O_3 nanoparticles: A DFT study

Elham Mohammad-Hasani, S Ali Beyramabadi* & Mehdi Pordel

Department of Chemistry, Mashhad Branch, Islamic Azad University, Mashhad, Iran

Email: beiramabadi@yahoo.com; beiramabadi6285@mshdiau.ac.ir

Received 22 October 2016; revised and accepted 31 May 2017

The structural parameters, energetic behavior and natural bond orbital analysis of flucytosine, as well as its tautomerization mechanism are explored theoretically using density functional theory calculations. The PCM model has been adopted to consider the solvent effects. Due to the large HOMO-LUMO energy gap, the flucytosine molecule is highly stable. The non-covalent interactions of the most stable tautomer of flucytosine with the armchair (5,5) single wall carbon nanotube and the magnetic γ-Fe_2O_3 nanoparticle have been explored. In each case, the most stable form is determined. Intramolecular hydrogen bonds play an essential role in stability of the non-covalent interactions between the flucytosine molecule and the γ-Fe_2O_3 nanoparticle.

Keywords: Theoretical chemistry, Density functional theory calculations, Non-covalent interactions, Polarizable continuum model, Nanoparticles, Carbon nanotubes, Flucytosine, Iron oxide

Flueytosine (chemically 5-fluorocytosine), a fluoropyrimidine drug, is an antimycotic agent used in treatment of many fungal infections.[1, 2] Several investigations have demonstrated its effectiveness in human Candida infections.[3-6] It is a safe and effective systemic drug for prophylaxis against fungi patients with large surface burns.[7] This fluorinated pyrimidine is effective in the treatment of the cryptococcus infection also.[8]

Density functional theory (DFT) methods are being widely applied in investigations on structure and energetic behavior of drugs.[9-13] Herein, combining DFT methods and the solvent effects with the polarizable continuum model (PCM), the structural parameters, energetic behavior, the natural bond orbital (NBO) analysis of the flueytosine drug as well as mechanism of its tautomerization are investigated theoretically. Due to the increasing use of nanotechnology in drug delivery, exploring the interaction of nanoparticles with the organic molecules is of great importance.[14-27] So far, the covalent and non-covalent interactions of various molecules with the carbon nanotubes and iron-oxide nanoparticles have been investigated theoretically.[20-24] In this work, non-covalent interactions of flueytosine with single wall carbon nanotubes and magnetic γ-Fe_2O_3 nanoparticles have been explored theoretically.

Computational methods

All of the calculations were performed using the Gaussian 03 software[28] by employing the B3LYP[29] functional of the density functional theory (DFT). The 6-311+G(d,p) basis set was used for investigation of the geometry, energetic behavior and tautomerism of the flueytosine molecule.

Interaction of the flueytosine drug with the carbon nanotubes and iron oxide nanoparticles (γ-Fe_2O_3) were investigated by using the B3LYP functional and 6-31G(d,p) basis sets for all of the atoms except for the Fe atoms, where the LANL2DZ basis sets was used with effective core potential (ECP) functions. The armchair (5,5) single wall carbon nanotube (SWCNT) was used, comprising 110 atoms (11.6 Å in length).

One of self-consistent reaction field methods, the sophisticated polarized continuum model (PCM)[30] was employed for investigation of the solvent effects in aqueous solution. First, all geometries were fully optimized. The optimized geometries were confirmed to involve no imaginary frequency, except for transition state (TS) that has only one imaginary frequency. The zero-point corrections and thermal corrections have been considered in evaluation of the energies. The optimized geometry was used to calculate the NBO analysis.

Results and discussion

The flucytosine drug can exist as six possible tautomers, geometries of which have been fully optimized in both of the gas phase and aqueous solution in PCM model. The PCM optimized geometries of the tautomers are shown in Fig. 1. As seen in Fig 1, the six tautomers of flucytosine can be tautomerized to each other via an intermolecular proton transfer (IPT) reaction. In comparison with the **F1** tautomer, in the **F2** tautomer the H4 proton

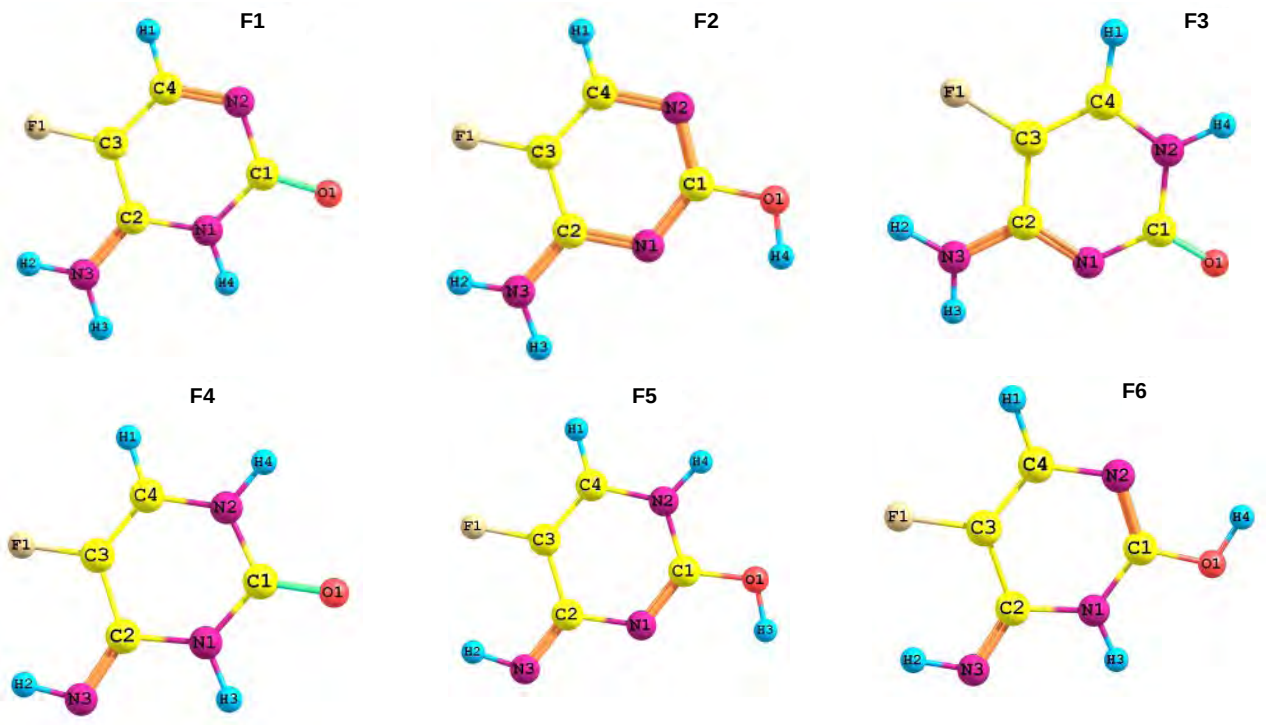

Fig. 1 – Optimized geometries for the six tautomers (**F1** to **F6**) of the flucytosine drug.

transfers from the N1 atom to the O1 carbonyl oxygen via an IPT. Further, the **F2** tautomer transformed to the **F3** tautomer by the IPT of the H4 atom from the O1 atom of the hydroxyl group to the N2 atom. Transfer of the H3 proton from the $-NH_2$ substituent to the N1 atom of the ring converts the **F3** tautomer to the **F4** tautomer. The IPTs of the H3 and H4 protons to the oxygen atom of the carbonyl group in the **F4** tautomer produce the **F5** and **F6** tautomers, respectively.

The relative energies of the six tautomers are gathered in Table 1, where the zero-point corrections have been considered in evaluation of electronic energies. As seen, the **F3** is the most stable tautomer of the flucytosine drug in aqueous solution. Tautomerization reaction of the **F3** tautomer to other tautomers has been investigated theoretically. The obtained barrier energies are gathered in Table 1.The most stable tautomer of flucytosine in aqueous solution is the **F3** tautomer, which can tautomerized to the **F2** and **F4** tautomers via the IPT of a proton to the next atom. However, tautomerization of the **F3** tautomer to the **F1** tautomer involves the IPT of a proton from the N1 atom to N3 atom. Due to jumping of proton to a farther atom, the **F3** $\rightarrow$ **F1** tautomerization involves higher activation energy than the **F3** $\rightarrow$ **F2** and **F3** $\rightarrow$ **F4** tautomerizations.

Table 1 – Relative energies of the investigated species

Species	Relative energy (kJ mol^{-1})	
	Gas phase	PCM model
F3	0.0	0.0
F2	-0.46	22.09
F1	31.29	21.86
F4	22.28	24.58
F5	73.54	89.21
F6	76.18	78.82
TS F3-F1	301.15	319.09
TS F3-F2	143.75	163.33
TS F3-F4	174.86	190.26

Important structural parameters of the optimized geometries are gathered in Table 2. As seen, in all of the tautomers, the flucytosine molecule has a planar geometry, where all of the substituents are in a same plane with the pyrimidine ring. The calculated structural parameters are in appropriate size.

The optimized geometry for the TS of the **F3** $\rightarrow$ **F2** tautomerization, named as **TSF3-F2** species, is shown in Fig 2, in which breaking of the N2-H4 bond together with the formation of O1-H4 bond is clear. The N2-H4 and O1-H4 bonds are 1.01 and 2.46 Å in the **F3** tautomer, respectively, which change to 0.96 and 3.06 Å in the **F2** tautomer. These distances are 1.29 and 1.35 Å in the **TSF3-F2**, respectively. Going

Table 2 – Selected bond lengths and bond angles for the optimized geometries

	F1	**F2**	**F3**	**F4**	**TSF3-F1**	**TSF3-F2**	**TSF3-F4**
Bond lengths (Å)							
C4-H1	1.08	1.08	1.08	1.08	1.08	1.08	1.08
C4-N2	1.33	1.34	1.36	1.38	1.37	1.34	1.36
N2-H4	3.26	3.06	1.01	1.01	1.40	1.29	1.01
N2-C1	1.36	1.32	1.40	1.38	1.42	1.36	1.41
C1-O1	1.23	1.35	1.23	1.22	1.19	1.29	1.23
C1-N1	1.41	1.33	1.36	1.38	1.43	1.32	1.36
N1-C2	1.35	1.34	1.32	1.40	1.36	1.34	1.37
C2-N3	1.33	1.34	1.34	1.28	1.33	1.34	1.31
N3-H2	1.00	1.00	1.00	1.02	1.00	1.00	1.01
N3-H3	1.00	1.00	1.00	2.49	1.00	1.00	1.38
C2-C3	1.39	1.41	1.43	1.45	1.41	1.42	1.42
C3-F1	1.36	1.35	1.35	1.35	1.35	1.34	1.35
C3-C4	1.38	1.37	1.35	1.34	1.37	1.37	1.35
N1-H4	1.01	2.26	3.26	3.23	1.39	2.94	3.21
O1-H4	2.43	0.96	2.46	2.50	2.75	1.35	2.49
N1-H3	2.59	2.52	2.50	1.01	2.53	2.50	1.33
Bond angles (°)							
F1-C3-C4	122.0	121.7	121.6	121.2	122.1	121.1	121.8
C3-C4-N2	124.3	121.8	118.3	119.9	119.6	117.2	120.5
C4-N2-C1	118.5	114.7	123.1	123.5	108.9	119.7	124.2
N2-C1-O1	124.8	115.1	118.8	123.0	128.1	104.5	120.6
N2-C1-N1	117.3	128.2	117.3	114.1	103.7	126.0	113.3
O1-C1-N1	117.7	116.6	123.8	123.0	127.4	129.3	126.1
C1-N1-C2	124.9	117.2	120.9	127.9	110.6	115.3	125.3
N1-C2-N3	121.1	119.4	119.5	119.5	120.0	118.6	118.8
C2-N3-H3	122.1	119.6	119.4	55.7	119.4	119.5	77.4
C2-N3-H2	119.8	121.2	121.4	110.3	121.2	121.4	123.6
N1-C2-C3	115.0	118.5	121.0	112.3	116.6	120.9	118.8
N3-C2-C3	123.8	122.0	119.3	128.2	122.8	120.4	137.5
C2-N1-H4	119.7	173.8	98.5	104.0	98.6	113.5	100.6
C2-N1-H3	52.0	53.8	54.0	116.5	52.9	54.3	76.8
C1-N1-H4	115.3	56.5	22.3	23.8	69.9	1.7	24.8
C1-O1-H4	58.1	107.8	56.9	54.2	14.5	75.2	56.0
Dihedral angles (°)							
F1-C3-C4-N2	179.9	-179.9	-179.9	180.0	179.8	-179.9	180.0
C3-C4-N2-C1	0.0	-0.0	-0.1	0.0	25.6	0.0	0.0
C4-N2-C1-N1	-0.1	0.0	0.07	-0.1	-66.5	-0.0	-0.0
C4-N2-C1-O1	179.9	-179.9	-179.9	179.9	121.7	179.9	180.0
N2-C1-N1-C2	0.0	-0.0	-0.0	0.1	68.5	0.0	-0.0
C1-N1-C2-N3	179.9	-179.9	-179.9	179.9	159.5	179.9	-179.9
N1-C2-N3-H3	0.0	0.0	0.0	0.0	-5.0	0.4	0.0
N1-C2-N3-H2	179.9	-179.9	-179.9	-180.0	166.4	179.6	-180.0
C1-N1-C2-C3	0.0	0.0	0.0	0.0	-27.7	0.0	0.0
N3-C2-C3-C4	179.9	179.9	179.9	-180.0	157.4	-179.9	179.9
N3-C2-C3-F1	0.0	0.0	0.0	0.0	-6.7	0.1	-0.0

from the **F3** tautomer to the **F2** tautomer, some structural parameters have changed, important of which are decrease in the C1-N2 and C4-N2 bond lengths and increase in the C1-O1 bond length of carbonyl group (Table 2).

The **TSF3-F4** is the optimized TS for the **F3** $\rightarrow$ **F4** tautomerization, optimized geometry of which is shown in Fig 2. As seen, breaking of the N3-H3 bond and formation of the N1-H3 bond are obvious. The N3-H3 and N1-H3 distances are 1.00 and 2.50 Å respectively in the **F3** tautomer., which change respectively to 2.49 and 1.01 Å in the **F4** tautomer and 1.38 and 1.33 Å in the **TSF3-F4** species.

The optimized geometry of the **TSF3-F1** (the TS of the **F3** $\rightarrow$ **F1** tautomerization) is shown in Fig 2, in which simultaneous cleavage of the N2-H4 bond and

Fig. 2 – Optimized geometries for the **TSF3-F1**, **TSF3-F2** and **TSF3-F4** species.

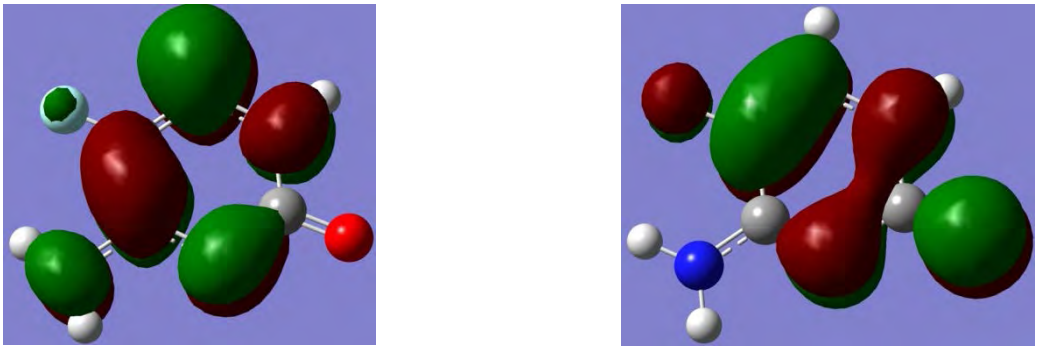

LUMO **HOMO**

Fig. 3 – HOMO and LUMO frontier orbitals of the **F3** tautomer of flucytosine.

formation of N1-H4 bond has occurred. The N2-H4 and N1-H4 distances are 1.01 and 3.26 Å for the **F3** tautomer, respectively, which are 3.26 and 1.01 Å in the **F1** tautomer. These distances are 1.40 and 1.39 Å in the optimized geometry of the **TSF3-F1** species, respectively. Important changes in structural parameters of the molecule during the **F3** $\rightarrow$ **F4** and **F3** $\rightarrow$ **F1** tautomerizations are listed in Table 2.

The **TSF3-F4** is the optimized TS for the **F3** $\rightarrow$ **F4** tautomerization, optimized geometry of which is shown in Fig 2. As seen, breaking of the N3-H3 bond and formation of the N1-H3 bond are obvious. The N3-H3 and N1-H3 distances are 1.00 and 2.50 Å respectively in the **F3** tautomer., which change respectively to 2.49 and 1.01 Å in the **F4** tautomer and 1.38 and 1.33 Å in the **TSF3-F4** species.

The optimized geometry of the **TSF3-F1** (the TS of the **F3** $\rightarrow$ **F1** tautomerization) is shown in Fig 2, in which simultaneous cleavage of the N2-H4 bond and formation of N1-H4 bond has occurred. The N2-H4 and N1-H4 distances are 1.01 and 3.26 Å for the **F3** tautomer, respectively, which are 3.26 and 1.01 Å in the **F1** tautomer. These distances are 1.40 and 1.39 Å in the optimized geometry of the **TSF3-F1** species, respectively. Important changes in structural parameters of the molecule during the **F3** $\rightarrow$ **F4** and **F3** $\rightarrow$ **F1** tautomerizations are listed in Table 2.

NBO analysis is a useful tool in computational chemistry, especially in identification of the chemical bonds and charge distribution if chemical compounds. The 3D-distribution map of the highest-occupied-molecular orbital (HOMO) and the lowest-unoccupied-molecular orbital (LUMO) of the **F3** tautomer of the flucytosine drug are shown in Fig. 3. The conjugation stabilizes the molecule of drug. Electron transfer from the HOMO to the LUMO orbital is a $\pi \rightarrow \pi^*$ transition.

The energy gap, energy difference between the HOMO and LUMO frontier orbitals is an important characteristic of the chemical compounds, which has a significant role in such cases as electronic spectra and photochemical reactions. Herein, the value of the energy gap between the HOMO and LUMO frontier orbitals of the **F3** tautomer of flucytosine is equal to 4.95 eV. This large value of energy gap exhibits that structure of flucytosine is very stable.[31, 32]

Nanocompounds are beneficial in many aspects of human life especially in drug delivery.[14-27] Herein, the

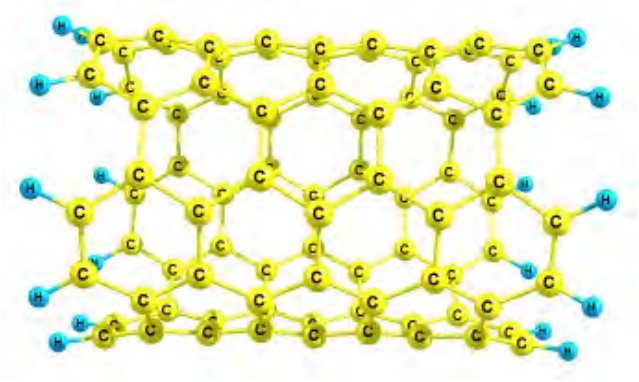

Fig. 4 – Optimized geometry of the armchair (5,5) single wall carbon nanotube (SWCNT).

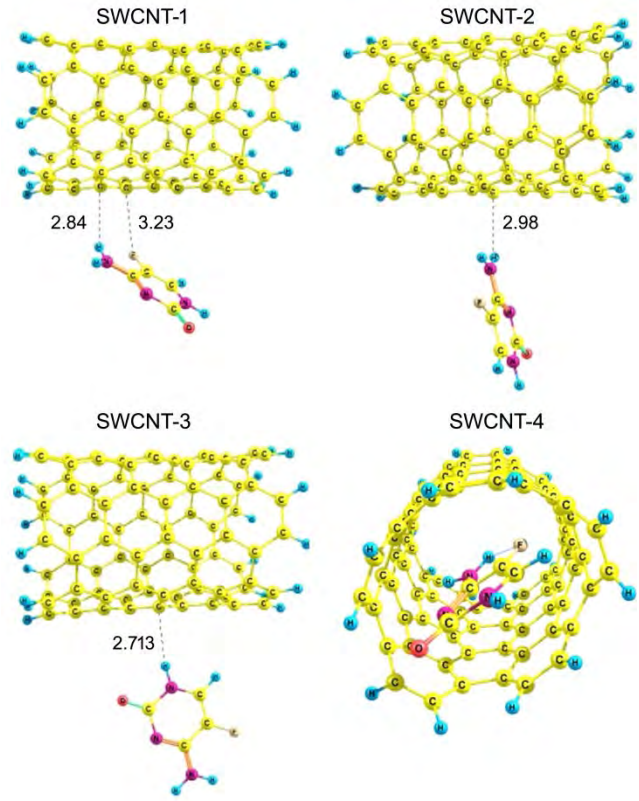

Fig. 5 – Optimized geometries of the four possible non-covalent interactions between the **F3** tautomer and the SWCNT.

non-covalent interactions of the **F3** tautomer of flucytosine with the carbon-nanotube and magnetic nanoparticles of γ-Fe_2O_3 have been investigated theoretically.

The armchair (5,5) single wall carbon nanotube (SWCNT) with 11.6 Å length has been used as a model for the carbon-nanotube. In Fig. 4, the optimized geometry of the SWCNT is shown. The **F3** tautomer

Table 3 – Electronic energy of the optimized geometries for non-covalent interactions of the F3 tautomer of flucytosine and SWCNT in aqueous solution with the calculated binding energies

Species	Electronic energy (Hartree)	Binding energy (kJ/mol)
SWCNT	-3441.799783	-
F3 tautomer	-494.1830078	-
SWCNT+F3 tautomer[a]	-3935.982791	-
SWCNT-1	-3935.984386	-4.18
SWCNT-2	-3935.983044	-0.66
SWCNT-3	-3935.984163	-3.60
SWCNT-4	-3935.984699	-5.00

[a]Sum of electronic energies of the free SWCNT and the F3 tautomer.

can interact with the SWCNT in different ways. In this work, four possible of the non-covalent interactions between the **F3** species and the SWCNT have been investigated, which are named as SWCNT-form1 to SWCNT-form4. Their optimized geometries are shown in Fig. 5.

In the SWCNT-1 form, the **F3** is roughly parallel with respect to the SWCNT. The fluoro and $–NH_2$ substituents are closer to the nanotube by about 3 Å. However, in the SWCNT-2 and SWCNT-3 forms, the **F3** species is perpendicular to the SWCNT; and the drug molecule interacts with the carbons of the SWCNT via hydrogen atoms of the $–NH_2$ substituent and –NH of the pyrimidine ring, respectively. The calculated distances between flucytosine and SWCNT are shown in Fig. 5. It is possible that the small molecule of the flucytosine drug is encapsulated inside the SWCNT. This phenomenon is seen in the SWCNT-4 form, wherein the drug molecule is inside the disordered SWCNT.

Calculated binding energies in aqueous solution are listed in Table 3. The binding energy is defined as: $\Delta E = E_{(SWCNT-*)} - (E_{(F3)} + E_{(SWCNT)})$, where the $E_{(SWCNT-*)}$, $E_{(F3)}$ and $E_{(SWCNT)}$ are the electronic energies of the investigated species, i.e., one of the four SWCNT-1 to SWCNT-4 forms, the **F3** tautomer and the free SWCNT, respectively. As seen in Table 3, the SWCNT-4 form involves the highest stability (the lowest energy) and is the most favorable form for the non-covalent interaction of flucytosine with the SWCNT.

The non-covalent interactions between the most stable tautomer of flucytosine (**F3**) and the the γ-Fe_2O_3 nanomagnetic particles have been investigated. A suitable model has been presented for γ-Fe_2O_3 nanoparticles on the basis of the $Fe_6(OH)_{18}(H_2O)_6$ ring cluster. This model is in good agreement with the experimental data such as the

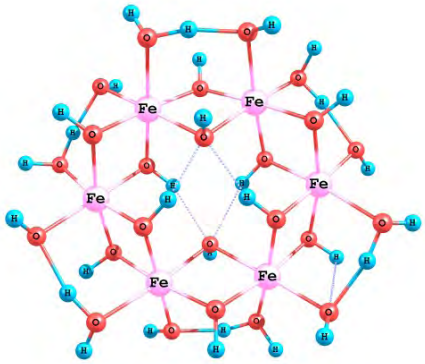

Fig. 6 – Optimized geometry of the γ-Fe_2O_3 nanoparticle.

Table 4 – The electronic energies of the optimized geometries for non-covalent interactions of the **F3** tautomer and γ-Fe_2O_3 nanoparticle in aqueous solution together with the binding energies

Species	Electronic energy (Hartree)	Binding energy (kJ/mol)
Nano-Fe_2O_3	-2654.5173599	-
F3 tautomer	-494.1830078	-
Nano-Fe_2O_3+ **F3** tautomer[a]	-3058.700368	-
NANO-Fe1	-3058.718510	-47.59
NANO-Fe2	-3058.700598	-0.61
NANO-Fe3	-3058.714624	-37.39

[a]Sum of electronic energies of the γ-Fe_2O_3 nanoparticle and the **F3** tautomer.

vibration frequencies and bond lengths.[23, 24] Optimized geometry of the used model for the γ-Fe_2O_3 is shown in Fig. 6.

For exploring non-covalent interactions of **F3** with the nanomagnetic γ-Fe_2O_3, the structure of the **F3**-γ-Fe_2O_3 species has been optimized in three different forms, designated as NANO-Fe1, NANO-Fe2 and NANO-Fe3; their optimized geometries are shown in Fig. 7. The calculated electronic energies and binding energies are gathered in Table 4.

In the NANO-Fe1 form, there are three hydrogen bonds. The oxygen atom of the carbonyl group is engaged in intramolecular H-bonds with the H atom of H_2O and –OH. Also, the hydrogen atom of the –NH amine group makes a strong H-bond with the oxygen atom of the –OH ligand, length of which is 1.73 Å. In the NANO-Fe1 form, the fluoro substituent is engaged in a weak H-bond interaction with the –OH ligand. This form involves two weak H-bonds (Fig. 7). In the NANO-Fe3 form, the nitrogen atom of the pyrimidine ring and proton of the $–NH_2$ substituent are engaged in a strong H-bond with the nanoparticles.

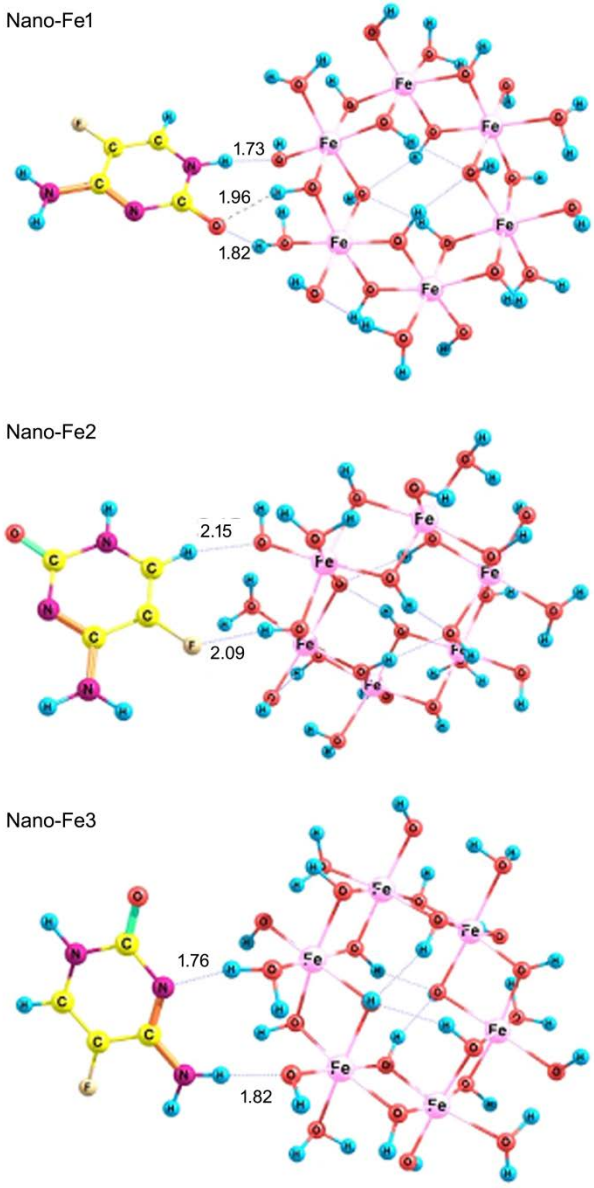

Fig. 7 – Optimized geometries of the three possible non-covalent interactions between the **F3** tautomer and the γ-Fe_2O_3 nanoparticle.

In Table 4, the DFT-computed binding energies in aqueous solution are listed. Herein, the binding energy is defined as: $\Delta E = E_{(NANO-Fe^*)} - (E_{(F3)} + E_{(Fe_2O_3)})$, where the $E_{(NANO-Fe^*)}$, $E_{(F3)}$ and $E_{(Fe_2O_3)}$ are the electronic energies of one of the three NANO-Fe forms, the **F3** tautomer of flucytosine and the optimized model of the γ-Fe_2O_3 nanoparticle, respectively. The NANO-Fe1 form involves three strong H-bonds. As expected, this form has the lowest energy and highest stability.

Hence, the NANO-Fe1 is the most suitable model for the non-covalent interaction of the **F3** tautomer of the flucytosine drug with the γ-Fe_2O_3 nanoparticle.

In this work, the geometries of the six-possible tautomers of flucytosine were optimized by the DFT calculations. In aqueous solution, the **F3** species is the most stable tautomer of flucytosine. The **F3** tautomer may be transformed to the other tautomers via IPTs. Tautomerism of flucytosine has been explored in both of the gas and solution phases. The tautomerization reactions have high barrier energy and tautomerization of the **F3** tautomer is an unfavorable reaction in the aqueous solution.

The NBO calculation on the **F3** tautomer showed that the conjugation stabilizes the molecule. High HOMO-LUMO energy gap confirms that the flucytosine molecule is stable.Also, the non-covalent interactions between the SWCNT nanotube and the **F3** tautomer of the flucytosine drug have been investigated in four proposed forms. The most stable form was the SWCNT-4 form, where the small molecule of the flucytosine drug is encapsulated inside the SWCNT. Also, the non-covalent interactions of the **F3** tautomer with the proposed model for the magnetic γ-Fe_2O_3 nanoparticles have been explored in three different forms. All the forms involve intermolecular H-bonds in their optimized geometry, between the –OH and H_2O ligands of the γ-Fe_2O_3 nanoparticle and H, O and N atoms of the flucytosine molecule. The NANO-Fe1 is the most stable form, which involves three strong H-bonds, with the H-bond interaction increasing the stability of the chemical compounds.

References

1 Chouini-Lalanne N, M C Malet-Martion M C, Martion R & Michel G, *Antimicrob Agents Chemother*, 33 (1989) 1939.
2 Grlrnberg E, Titsworth E & Bennett M, *Antimicrob Agents Chemother*, 3 (1963) 566.
3 Holt R J & Newman, R L, *J Clin Pathol*, 26 (1973) 167.
4 Davies R R & Reeves D S, *Br Med J*, 1 (1970) 577.
5 Schonebeck J, Steen L & Tarnuck A, *Scand J Urol Nephrol*, 6 (1972) 37.
6 Vandevelde A G, Mauce A A & Jounson J E, *Ann Intern Med*, 77 (1972) 43.
7 Richardson G L, Rabinovich S, Boyd W C & Hartford C E, *Burns*, 1 (1972) 113.
8 Fass J F & Perkins R L, *Ann Intern Med*, 14 (1971) 535.
9 Alkorta I & Elguero J, *J Mol Struct*, 1056–1057 (2014) 209.
10 Ramya T, Gunasekaran S & Ramkumaar G R, *Spectrochim Acta Part A*, 114 (2013) 277.
11 Zhu M & Zhou L, *Comput Theo Chem*, 1051 (2015) 24.
12 Rastogi V K & Alcolea Palafox M, *Spectrochim Acta Part A*, 79 (2011) 970.
13 Sadeghzade Z, Beyramabadi S A & Morsali A, *Spectrochim Acta Part A*, 138 (2015) 637.
14 Ma W & Fang Y, *J Nanopart Res*, 8 (2006) 761.
15 Farhadi S, Mahmoudi F & Simpson J, *J Mol Struct*, 1108 (2016) 583.
16 Anuratha M, Jawahar A, Umadevi M, Sathe V G, Vanelle P, Terme T, Khoumeri O, Meenakumari V & Milton Franklin Benial A, *Spectrochim Acta Part A*, 149 (2015) 558.
17 Tao Z & Fang Y, *J Mol Struct*, 797 (2006) 40.
18 Wang Y, Liu S, Liu Z, Yang J & Hu X, *Spectrochim Acta Part A*, 105 (2013) 612.
19 Gobal F, Arab R & Nahali M, *J Mol Struct*, 959 (2010) 15.
20 De Souza L A, Nogueira C A S, Ortega P F R, Lopes J F, Calado H D R, Lavall R L, Silva G G, Dos Santos H F & De Almeida W B, *Inorg Chim Acta*, 447 (2016) 38.
21 Soltani Azmoodeh A, Bezi Javan M, Lemeski E T & Karami L, *Appl Sur Sci*, 384 (2015) 230.
22 Mansoorinasab A, Morsali A, Heravi M M & Beyramabadi S A, *J Comput Theor Nanosci*, 12 (2015) 4935.
23 Heshmati Jannat Maghama A, Morsali A, Eshaghi Z, Beyramabadi S A & Chegini H, *Prog React Kinet Mech*, 40 (2015) 119.
24 Haghtalab T & Soleymanabadi H, *Indian J Chem*, 55A (2016) 657.
25 Jayarathne L, Ng W J, Bandara A, Vitanage M, Dissanayake C & Weerasooriya R, *Colloids Surf A*, 403 (2012) 96.
26 Jalayeri E, Morsali A & Bozorgmehr M R, *Indian J Chem*, 55A (2016) 1202.
27 Arikrishnan J, Sheerin S K, Tabasum Murugavelu M & Karthikeyan B, *Indian J Chem*, 50A (2011) 46.
28 *Gaussian 03, Revision B.03*, (Gaussian, Inc.,Pittsburgh PA) 2003.
29 Lee C, Yang W & Parr R G, *Phys Rev B*, 37 (1988) 785.
30 Tomasi J & Cammi R, *J Comput Chem*, 16 (1995) 1449.